

Preparation and Corrosion Resistance of poly(o-toluidine)/nano SiC/epoxy Composite Coating

Jiwei Huang^{1,2,3}, Chuanbo Hu^{1,*}, Yongquan Qing¹

¹ School of Biological and Chemical Engineering, Guangxi University of Science and Technology, Liuzhou 545006, China

² Guangxi Key Laboratory of Green Processing of Sugar Resources, Guangxi University of Science and Technology, Liuzhou 545006, China

³ Key Laboratory for Processing of Sugar Resources of Guangxi Higher Education Institutes, Guangxi University of Science and Technology, Liuzhou 545006, China

*E-mail: huchuanbo@126.com

Received: 30 September 2015 / Accepted: 25 October 2015 / Published: 4 November 2015

In the presence of nano silicon carbide (SiC) particles, using o-toluidine monomer as raw material and ammonium persulfate as the oxidant, the poly(o-toluidine)/nano SiC composite was prepared by in situ polymerization method. Fourier transformation infrared spectroscopy (FT-IR), UV-visible spectroscopy (UV-vis), X-ray diffraction (XRD) and Scanning electron microscopy (SEM) were used to characterize the composition and structure of the composite. Poly(o-toluidine) or poly(o-toluidine)/nano SiC composite fillers were mixed with epoxy resin through a solution mixing method and the composite coatings were coated onto the surface of iron coupons. The corrosion resistance of the composite coatings was evaluated by electrochemical measurements in 3.5% NaCl solution as corrosion environment. The results obtained showed that poly(o-toluidine)/nano SiC composite containing coatings has got higher corrosion resistance than that of poly(o-toluidine). The enhancement of corrosion protection efficiency of poly(o-toluidine)/nano SiC composite containing coating is due to the formation of more uniformly passive film on iron surface and the addition of nano SiC particles increase the tortuosity of the diffusion pathway of corrosive substance.

Keywords: Poly(o-toluidine)/nano SiC composite; Poly(o-toluidine); Corrosion resistance; Electrochemical measurements; Passive film

1. INTRODUCTION

The use of conducting polymers for the control of metals against corrosion is an area which is gaining increasing attention. Among the conducting polymers, the derivatives of polyaniline (PANI) have been gaining particular attention due to their excellent corrosion protection properties [1,2]. It has

been reported that the derivatives of PANI have remarkable capability to protect stainless steel and Cu from corrosion [3–5].

The literatures [6–8] have been investigated that the electronic-donating group substituent of PANI derivatives can be achieved more significant improvement in the corrosion protection properties. Benchikh et al. [9] found that soluble PANI derivatives such as poly(*o*-toluidine) (POT) and poly(aniline-co-*ortho*toluidine) have been considered as organic inhibitors that can reduce the corrosion rate of steel in 3.0% NaCl solution. As a major derivative of aniline, *o*-toluidine (OT) is substituted by electron-donating group ($-\text{CH}_3$), has been extensively used in the synthesis of dye, pesticide, pharmaceutical and organic intermediates.

Generally, the inorganic additives play an important role in the improvement of polymers matrix properties, such as thermal, mechanical, electrical conductivity and corrosion protection properties [10–12]. Mostafaei et al. [13] prepared PANI/ZnO nanocomposite by in situ chemical oxidative method, the electrochemical measurements found that PANI/ZnO nanocomposite containing coating has got higher corrosion resistance than that of PANI in 3.5% NaCl solution. The inorganic nanoparticles such as SiC possess a good chemical stability, high strength and microhardness, low friction coefficient, good wear resistance and corrosion resistance at extreme environments [14]. Shi et al. [15] prepared Ni–Co/SiC nanocomposite coatings by electrodeposition method, and found that the Ni–Co/SiC nanocomposite coating with better corrosion resistance may be ascribed to the favorable chemical stability of nano SiC particles, which contributing to reduce the hole size in the composite coatings and to prevent the corrosion pits from growing up. In this paper, poly(*o*-toluidine)/nano SiC composite were prepared by in situ polymerization method in hydrochloric acid (HCl) medium, and using of this composite in the preparation of a poly(*o*-toluidine)/nano SiC/epoxy composite coating. The corrosion resistance of poly(*o*-toluidine)/nano SiC/epoxy composite coating was investigated by potentiodynamic polarization and electrochemical impedance spectroscopy (EIS) in 3.5 % NaCl solution as corrosion environment, and was also compared with that of poly(*o*-toluidine)/epoxy composite coating and pure epoxy coating.

2. EXPERIMENTAL

2.1 Materials

o-toluidine, ammonium persulfate (APS), hydrochloric acid (HCl), ammonium hydroxide ($\text{NH}_3\cdot\text{H}_2\text{O}$), sodium chloride (NaCl), butyl alcohol, dibutyl phthalate, ethanol, ethyl acetate and *N*-methyl-2-pyrrolidone (NMP) were analytical grade and used as received. Epoxy resin (EP) and polyamide (low molecular weight 650) were obtained from Yichun Yuanda Chemical Co., Ltd. Nano SiC particles with particle size of 40 nm were obtained from Shanghai Chaowei Nano Technology Co., Ltd. All other chemicals were commercially available and used as received.

2.2 Preparation of poly(o-toluidine)/nano SiC composite powders

Poly(o-toluidine)/nano SiC composite powders (POT/SiC) were prepared by in situ polymerization method, o-toluidine was distilled to colorless before to use. For this preparation, 80 mL of 1.0 mol/L HCl was added to 8.50 mL of o-toluidine monomer, 0.65 g of nano SiC particles was dispersed in o-toluidine hydrochloride solution by ultrasound, then the mixed solution were added to the three mouth flask and magnetic stirring for 30 min, to obtain the uniform dispersion of gray green solution. 18.26 g of APS as oxidant was dissolved in 120 ml of 1.0 mol/L HCl and the solution was added dropwise to the above mixture solution under vigorous stirring in an ice bath, the polymerization temperature less than 5 °C was maintained for 6 h to complete the preparation process. The products was filtered and washed several times with ethanol and deionized water until the filtrate became colorless, and then were dried in a vacuum oven at 60 °C for 20 h. The final POT/SiC composite in base form were received by immersed the above HCl-doped POT/SiC composite into 400 mL of 1.0 mol/L NH₃·H₂O solution under magnetically stirring for 3 h at room temperature, followed by re-filtered, washed and dried. Pure POT was also prepared in an exactly similar method without the using of nano SiC particles in order to compare the structure and corrosion resistance with POT/SiC composite.

2.3 Characterization of powders

The FT-IR spectra of the samples were recorded using a Nicolet 380 spectrometer by the KBr pellet technique in the range of 4000~500 cm⁻¹. The UV-vis spectra of the samples were recorded using a UV-2102PC spectrophotometer in the range of 200~850 nm, the samples were prepared by dissolving small a amount of a powder in NMP solution. The XRD spectra of the samples were recorded using a DX-2700 X-ray diffraction in the range of 10°~90°. The SEM images of the samples were recorded using a S-3400N digital scanning electron microscopy.

2.4 Preparation of composite coatings onto the iron substrate

The iron coupons with 3.5 cm×3.5 cm dimensions were used in corrosion studies. To remove any existing passive films and obtain a completely smooth surface, the iron coupons were mechanically polished using 320 and 600 grade emery papers respectively, followed by rinsing with acetone and ethanol, and then air-dried at room temperature before to use. As the only fillers, POT or POT/SiC composite powders were dispersed in epoxy and polyamide system by ultrasound, the fillers concentration was 5.0 mass%. The mixture solution of butyl alcohol and NMP was used as the solvent, dibutyl phthalate was used as the plasticizer and ethyl acetate was used as the defoaming agent. The composite coatings were directly coated onto the iron coupons substrate by using a brush coating method and cured at room temperature for 24 h after being cured at 60 °C for 12 h. Uncoated iron coupon was used as reference samples to comparison corrosion resistance with pure epoxy coating (EP coating), POT/epoxy composite coating (POT/EP composite coating) and POT/SiC/epoxy composite coating (POT/SiC/EP composite coating). The total thickness of the coating was 100±5 μm. Figure 1

shows the schematic preparation of poly(o-toluidine)/nano SiC/epoxy composite coating onto the iron substrate.

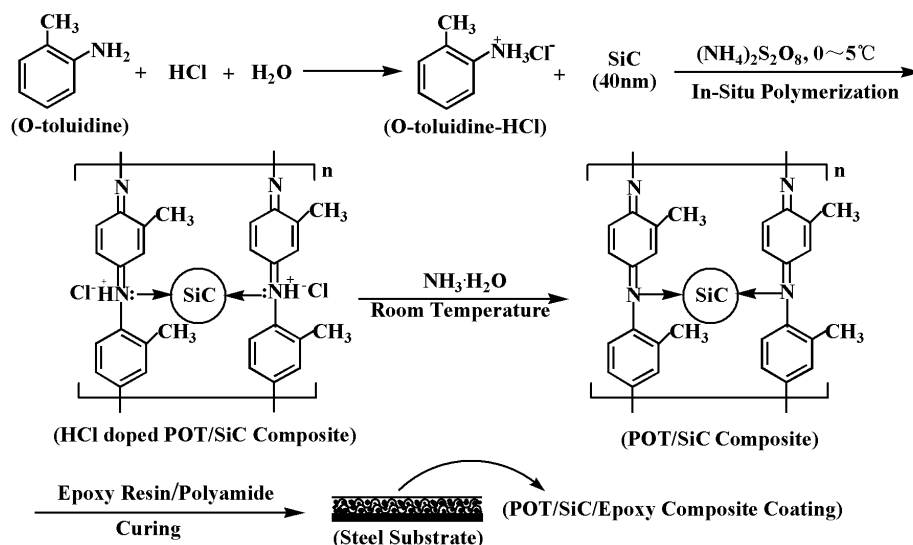


Figure 1. Schematic preparation of poly(o-toluidine)/nano SiC/epoxy composite coating

2.5 Evaluation of corrosion resistance of the coatings

Adopt the test methods of electrochemical corrosion to evaluate the corrosion resistance of different coatings in 3.5% NaCl solution by using a CHI660D electrochemical analyzer. Potentiodynamic polarization and electrochemical impedance spectroscopy (EIS) were recorded for uncoated and coated iron coupons by using a three-electrode electrochemical cell with saturated calomel electrode (SCE) as reference electrode and platinum gauze as counter electrode, the uncoated and coated iron coupons were used as working electrodes. EIS were measured at the frequency range of 100 kHz~10 mHz with an AC amplitude of 10 mV, potentiodynamic polarization curves were measured between $-1.2\sim 0.2$ V (vs SCE) at a scan rate of 5 mV/s.

3. RESULTS AND DISCUSSION

3.1 FT-IR characterization

The FT-IR spectra of nano SiC, POT and POT/SiC composite are shown in Figure 2. It is clearly observed that the FT-IR characteristic absorption peaks of POT with the literatures are consistent [16–18]. The peak at 2913 cm^{-1} is attributed to the C–H stretching of methyl group. The peaks at 1597 cm^{-1} and 1493 cm^{-1} are attributed to the C=C stretching vibrations of quinoid and benzenoid rings in POT chains, respectively. The peaks at 1302 cm^{-1} and 3395 cm^{-1} are attributed respectively to the C–N and N–H stretching vibration of linked with benzenoid rings. The peak at 1161 cm^{-1} is attributed to C–H plane stretching vibration of quinoid rings and the peak at 816 cm^{-1} is

attributed to C–H out plane bending vibration of benzenoid rings. From Fig. 2c, it can be seen that the characteristic absorption peaks of POT/SiC composite centered at around 3382, 2908, 1593, 1492, 1299, 1158 and 811 cm^{-1} , and all the absorption peaks related to POT have been shifted to lower wave numbers, which may be attributed to the incorporation of nano SiC particles into the POT matrix causing certain physicochemical interaction existed between POT and nano SiC particles. The certain physicochemical interaction may be the hydrogen bond [19]. Fig. 2a the FT-IR spectra of nano SiC shows that the characteristic absorption peaks centered at 816 cm^{-1} and 3440 cm^{-1} . Because the interaction existed between POT molecules and nano SiC, and the similar absorption peaks at the wave numbers existed in POT chains. These results suggest that the characteristic peaks of nano SiC turned to be weak or overlapped with characteristic peaks of POT.

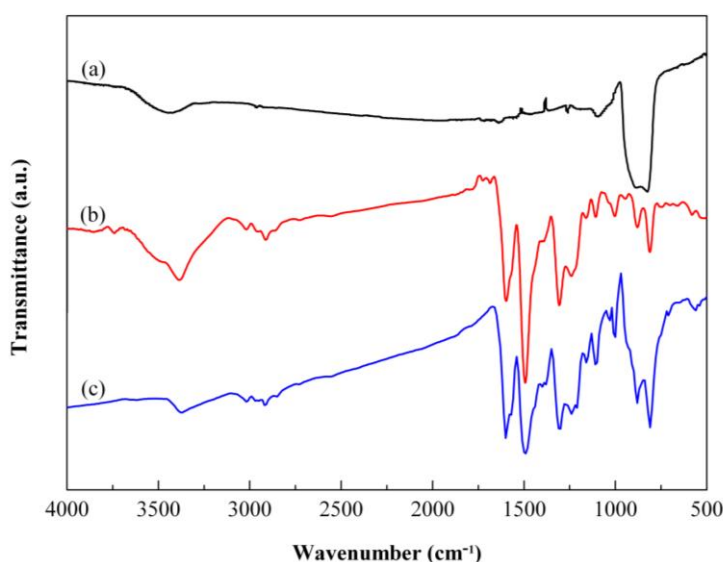


Figure 2. FT-IR spectra of (a) nano SiC, (b) POT and (c) POT/SiC composite powders

3.2 UV-vis characterization

The UV-vis spectra of POT and POT/SiC composite are shown in Figure 3. Fig. 3a shows that the two characteristic peaks of POT appear at around 311 nm and 615 nm, which are attributed to π - π^* transition of the benzenoid rings and n - π^* excitonic transition of benzenoid to quinoid rings [20,21], respectively. From Fig. 3b, it can be found that the shape of UV-vis spectra of POT/SiC composite is similar to POT and the corresponding absorption peaks are blue shifted to 309 nm and 608 nm, respectively. The intensity of absorption peaks are corresponding increased. These results indicate that some interactions existed between nano SiC particles and POT molecules. The wavelength increased due to the interaction between nano SiC and $-\text{NH}$ in POT molecules, thereby affecting the regularity and conjugated degree of POT molecule chains. This result is in a good agreement with FT-IR spectra of POT/SiC composite.

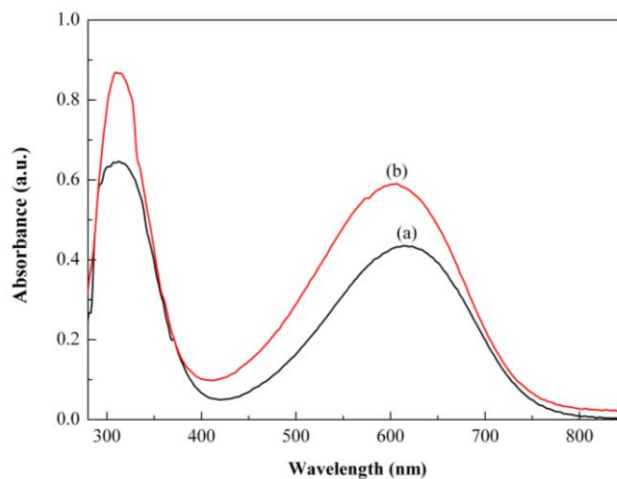


Figure 3. UV-vis spectra of (a) POT and (b) POT/SiC composite powders

3.3 XRD characterization

The XRD pattern of nano SiC, POT and POT/SiC composite are shown in Figure 4. From Fig. 4a, it can be seen that the XRD pattern of nano SiC shows sharp and well defined peaks indicating the crystalline nature of nano SiC, the observed 2θ values are consistent with the standard JCPDS values (JCPDS No. 29–1129). From Fig. 4b, it can be clearly seen that POT exhibits a single broad diffraction peaks at 2θ values around 20° , which is the characteristic diffraction peak of POT, it indicates that POT is amorphous. When nano SiC particles are incorporated into POT matrix, it can be seen that the XRD pattern of POT/SiC composite is very similar to that of nano SiC and POT, just only the broad diffraction peaks of POT turns weak and the intensity of diffraction peaks of POT/SiC composite are lower than that of nano SiC. It implies that POT deposited on the surface of nano SiC particle has no effect on the crystalline structure of nano SiC, the presence of noncrystalline POT reduces the mass-volume percentage of nano SiC and sequentially weakens diffraction peaks of nano SiC [22].

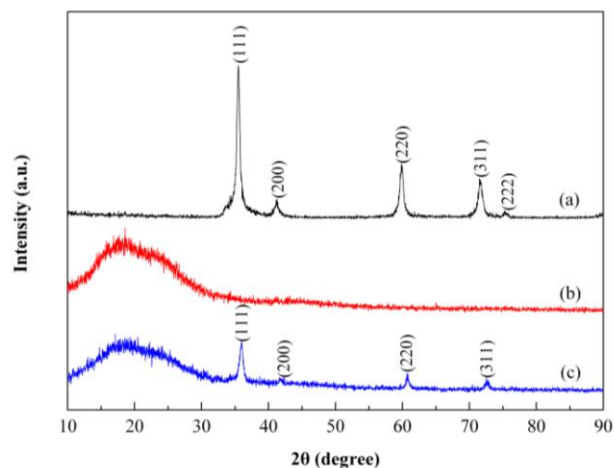


Figure 4. XRD patterns of (a) nano SiC, (b) POT and (c) POT/SiC composite powders

3.4 SEM characterization

The SEM images of nano SiC, POT and POT/SiC composite are shown in Figure 5. It can be seen that POT shows a floccule structure formed into irregular agglomerations, these materials connect with each other and create air-filled cavities which leads the compactness was poor. When nano SiC particles are dispersed in the reaction system act as the reaction cores, the adsorption of o-toluidine on the surface of nano SiC particles occurs and subsequent formation of POT. From Fig. 5c, it can be seen that the crystals of nano SiC particles are fully covered by POT in the case of POT/SiC composite and the composite shows a globular structure consisting of small globules and pores. This result indicates that nano SiC particles are encapsulated into the POT matrix can significantly improve the compactness of polymer.

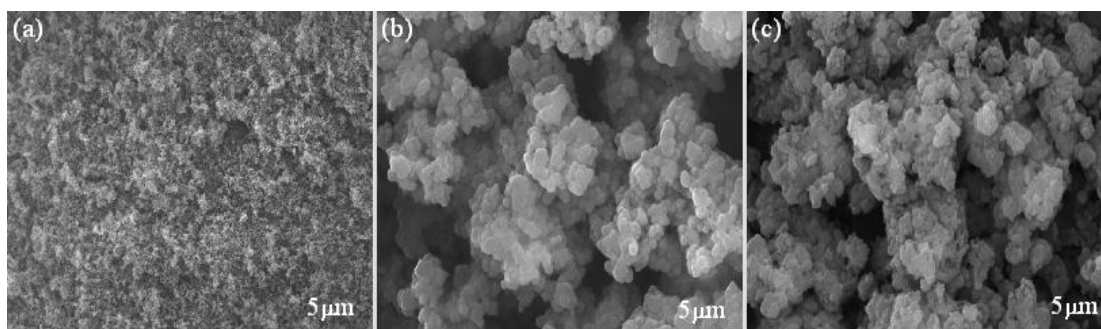


Figure 5. SEM images of (a) nano SiC, (b) POT and (c) POT/SiC composite powders

3.5 Corrosion resistance of the coatings

The corrosion resistance of pure epoxy coating, POT/EP composite coating and POT/SiC/EP composite coating were investigated in 3.5% NaCl solution as corrosion environment using potentiodynamic polarization measurement and electrochemical impedance spectroscopy (EIS) measurement.

3.5.1 Potentiodynamic polarization measurement

The potentiodynamic polarization measurement was performed to evaluate the corrosion resistance of the three coatings on iron substrates. The potentiodynamic polarization curves for coated iron coupons were recorded by sweeping of the potential from equilibrium potential toward negative and positive potentials against SCE reference electrode in 3.5% NaCl solution. The corrosion potential (E_{corr}), corrosion current density (I_{corr}), corrosion rate (V_{corr}), and polarization resistance (R_p) values of coated iron coupons calculated are based on the Tafel extrapolation method [23,24]. Extrapolation of these curves to their points of intersection provides both the E_{corr} and I_{corr} values. Generally, a higher E_{corr} and R_p , a lower I_{corr} and V_{corr} indicate better corrosion protection properties. The R_p values were

calculated from the potentiodynamic polarization curves, according to the Stern-Geary equation [25,26]:

$$R_p = \frac{b_a b_c}{2.303(b_a + b_c)I_{corr}}$$

Where, I_{corr} is determined by an intersection of the linear portions of the anodic and cathodic sections of the potentiodynamic polarization curves, and b_a and b_c ($\Delta E/\Delta \log I$) are anodic and cathodic Tafel slopes, respectively. The uncoated and coated iron coupons immersed in 3.5% NaCl solution for a few days before to test. The potentiodynamic polarization curves of uncoated and coated iron coupons are shown in Figure 6, the E_{corr} , I_{corr} , V_{corr} and R_p values of uncoated and coated iron coupons are shown in Table 1.

From Fig. 6 and Table 1, it can be seen that the E_{corr} values of POT/SiC/EP composite coating are higher than that of POT/EP composite coating, pure epoxy coating and uncoated iron coupon, and positive shifted about 108, 253 and 432 mV, respectively. The I_{corr} and V_{corr} values of POT/SiC/EP composite coating are lower than that of POT/EP composite coating, pure epoxy coating and uncoated iron coupon about 3, 10 and 118 times, respectively. The R_p values of POT/SiC/EP composite coating are higher than that of POT/EP composite coating, pure epoxy coating and uncoated iron coupon about 3, 12 and 159 times, respectively. In addition, the higher b_a values as compared to b_c values indicates that the application of the external current strongly polarizes the anode [27]. From Table 1, it can be seen that POT/SiC composite coating inhibit more the anodic and cathodic reactions, this result indicates that POT/SiC composite containing coating coated onto iron coupon surface influence the b_a values, as a consequence the anodic dissolution was decelerated.

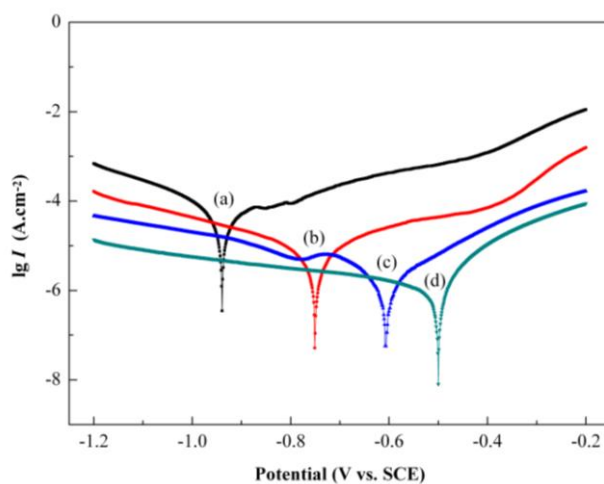


Figure 6. The potentiodynamic polarization curves of (a) uncoated iron coupon, (b) EP coating, (c) POT/EP composite coating and (d) POT/SiC/EP composite coating

Undoubtedly, POT/SiC/EP composite coating has a higher E_{corr} and R_p values but a lower I_{corr} and V_{corr} values. It indicates that the corrosion resistance of POT/SiC/EP composite coating is better than that of other two kinds of coated iron coupons. The mechanism of the enhanced corrosion protection effect of POT/SiC/EP composite coating is a result of the well dispersed nano SiC particles

incorporated into POT matrix that obviously improved the barrier properties of polymer, and it is also known that POT protects metal substrate against corrosion by its electrochemical protection mechanism, which the formation of Fe_3O_4 and $\gamma\text{-Fe}_2\text{O}_3$ as precursors of a passive layer to protect the underlying metal [28,29]. When POT/SiC composite fillers dispersed in epoxy and polyamide system, POT/SiC/EP composite coating containing three different materials and enjoying the combined properties, it act as a fence structure that block the diffusion of corrosion substances. So it is very effective in the protection of underlying iron coupon.

Table 1. Corrosion potential, corrosion current density, corrosion rate and polarization resistance of coated samples in 3.5% NaCl solution evaluated by potentiodynamic polarization measurement

Samples	E_{corr} (mV vs. SCE)	I_{corr} (A/cm^2)	v_{corr} (mm/year)	b_a (V/dec)	b_c (V/dec)	R_p ($\text{k}\Omega\cdot\text{Cm}^2$)
Uncoated iron coupon	-932	3.09×10^{-5}	3.62×10^{-1}	0.12	0.08	0.69
EP coating	-753	2.39×10^{-6}	2.80×10^{-2}	0.12	0.10	9.02
POT/EP composite coating	-608	6.60×10^{-7}	7.72×10^{-3}	0.13	0.12	41.05
POT/SiC/EP composite coating	-500	2.63×10^{-7}	3.08×10^{-3}	0.14	0.13	109.76

3.5.2 EIS measurement

The EIS measurement was also performed to evaluate the corrosion resistance of the different coatings on the iron coupon surface. The EIS curves of uncoated and coated iron coupons immersed in 3.5% NaCl solution for a period of time are shown in Figure 7. It is possible to use the diameter of the partially formed semicircle in EIS curves as an indicator of the corrosion rate [6,30–31]. Generally, larger diameter values point to slower corrosion rate and higher corrosion protection properties. It can be observed from Fig. 7 that the EIS curves of all iron coupons display similar characteristics, a depressed semicircle in the high frequency regions and no diffusion impedance in the low frequency regions. The diameter of EIS curves (a–d) shows that the diameter of POT/SiC/EP composite coating is the largest and the uncoated iron coupon is the lowest, which means the corrosion resistance of POT/SiC/EP composite coating is the best. This result is in accordance with potentiodynamic polarization measurement.

For uncoated iron coupon, because it has no protection layer, the EIS curve is characteristic of a system undergoing dissolution with the precipitation of a corrosion film on the iron surface, resulting in the resistance values is the lowest. For pure epoxy coating, the epoxy resin has a certain corrosion protection ability, but the poor barrier properties of the epoxy coating without any filler, the small molecules (oxygen and water) or ions can easily penetrate epoxy coating film and freely corrode the iron surface, resulting in a low resistance values. POT/EP composite coating containing POT fillers, the increased resistance values could be due to the passivation and barrier effects of POT, which maintains the potential of the iron coupon in the passive region [32], and the interactions of polar groups between POT fillers and epoxy resin can facilitate greater adsorption on iron surface. This

result indicates that the POT fillers dispersed in the epoxy and polyamide system, the composite coating have a greater capability of forming uniform compact adsorbed layer over iron substrate and decrease the effective area for corrosion reaction by blocking the reaction sites. Fig. 7d shows that POT/SiC/EP composite coating has got higher corrosion protection properties than POT/EP composite coating. The better corrosion protection properties of POT/SiC composite containing coating than that of POT is due to its relative good dispersity so that it can be dispersed uniformly in epoxy and polyamide system which can facilitate to maintain the passive layer uniformly on the iron surface. Furthermore, this is also due to the barrier properties of nano SiC particles, which could more effectively increase the tortuosity of the diffusion pathway of oxygen, water and chloride ions.

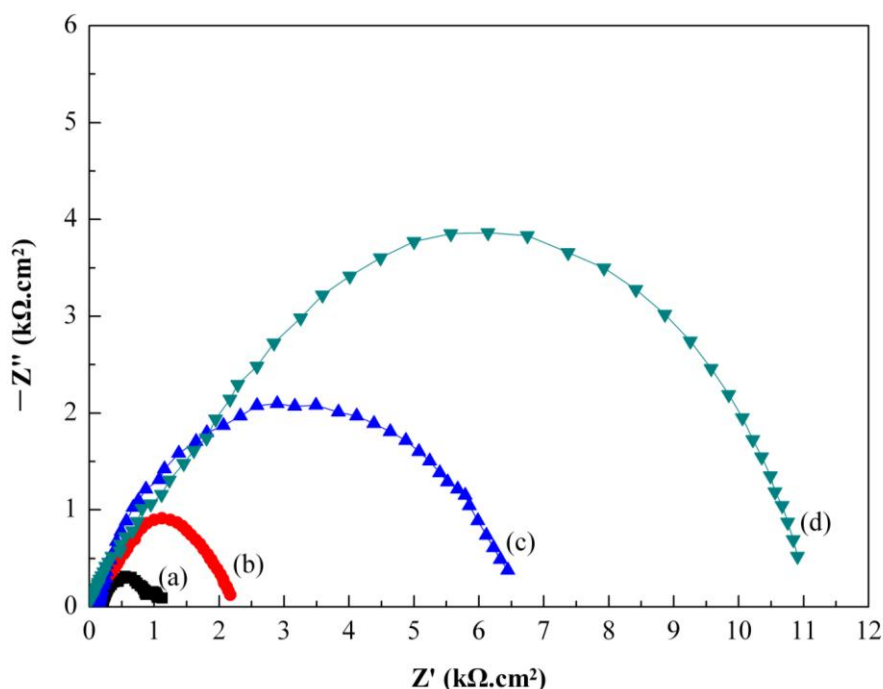


Figure 7. EIS curves of (a) uncoated iron coupon, (b) EP coating, (c) POT/EP composite coating and (d) POT/SiC/EP composite coating

4. CONCLUSIONS

Poly(o-toluidine)/SiC composite has been successfully preparation by in situ polymerization method in the presence of o-toluidine monomer and nano SiC particles using ammonium persulfate as oxidant in hydrochloric acid medium. FT-IR spectra and UV-vis spectra indicate that some interaction exists between POT chains and nano SiC particles. XRD patterns indicate that the crystalline performance of nano SiC particles is not effect by POT. SEM images indicate that nano SiC particles are evenly dispersed in POT matrix, and significantly improve the compact structure of POT molecules. The corrosion studies of all coated iron coupons in 3.5% NaCl solution by electrochemical measurements have shown that POT/SiC/EP composite coating has got higher corrosion resistance than that of POT/EP composite coating and pure epoxy coating. The higher corrosion protection

properties of epoxy coating containing POT/SiC composite fillers has been associated with increase in the barrier and passivation effects.

ACKNOWLEDGEMENTS

The authors are grateful for the financial support of the Innovation Project of Guangxi Graduate Education (Grant No. YCSZ2014202), and the authors are also thankful to Guangxi University of Science and Technology providing the facilities for the research.

References

1. L. Ma, C. Q. Huang and M. Y. Gan, *J. Appl. Polym. Sci.*, 127 (2013) 3699
2. C. J. Xing, Z. M. Zhang, L. M. Yu, L. J. Zhang and G. A. Bowmaker, *RSC. Adv.*, 4 (2014) 32718
3. B. Duran, G. Bereket, M. C. Turhan and S. Virtanen, *Thin. Solid. Films*, 519 (2011) 5868
4. B. Duran, M. C. Turhan, G. Bereket and A. S. Saraç, *Electrochim. Acta*, 55 (2009) 104
5. S. Bilal, S. Farooq, A. A. Shah and R. Holze, *Synthetic. Met.*, 197 (2014) 144
6. E. Hür, G. Bereket and Y. Şahin, *Curr. Appl. Phys.*, 7 (2007) 597
7. H. F. Hu, M. Y. Gan, J. Yan, L. Ma and C. Q. Ge, *Prog. Org. Coat.*, 81 (2015) 87
8. Z. T. Li, L. Ma, M. Y. Gan, J. Yan, H. F. Hu, J. Zeng and F. F. Chen, *Polym. Compos.*, 34 (2013) 740
9. A. Benchikh, R. Aitout, L. Makhloufi, L. Benhaddad and B. Saidani, *Desalination*, 249 (2009) 466
10. A. Olad and R. Nosrati, *Prog. Org. Coat.*, 76 (2013) 113
11. S. Radhakrishnan, C.R. Siju, D. Mahanta, S. Patil and G. Madras, *Electrochim. Acta*, 54 (2009) 1249
12. M. G. Hosseini, M. Jafari and R. Najjar, *Surf. Coat. Technol.*, 206 (2011) 280
13. A. Mostafaei and F. Nasirpour, *Prog. Org. Coat.*, 77 (2014) 146
14. V. Presser, K. G. Nickel, O. Krummhauser and A. Kailer, *Wear*, 267 (2009) 168
15. L. Shi, C. F. Sun, P. Gao, F. Zhou and W. M. Liu, *Appl. Surf. Sci.*, 252 (2006) 3591
16. V. V. Chabukswar, A. S. Horne, S. V. Bhavsar, K. N. Handore, P. K. Chhattise, S. S. Pandule, D. T. Walunj, S. U. Shisodia, A. Citterio, S. Dallavalle, K. C. Mohited and V. B. Gaikwad, *J. Macromol. Sci., Part A: Pure Appl. Chem.*, 51 (2014) 435
17. S. Poyraz, Z. Liu, Y. Liu, N. Lu, M. J. Kim and X. Y. Zhang, *Sens. Actuators. B*, 201 (2014) 65
18. J. Liu, X. H. Wen, Z. P. Liu, Y. Tan, S. Y. Yang and P. Zhang, *Colloid. Polym. Sci.*, 293 (2015) 1391
19. J. L. Gu, L. Ma, M. Y. Gan, F. Zhang, W. L. Li and C. Q. Huang, *Thermochim. Acta*, 549 (2012) 13
20. A. Zehhaf, E. Morallon and A. Benyoucef, *J. Inorg. Organomet. Polym.*, 23 (2013) 1485
21. S. A. Kumar, A. P. Singh, P. Saini, F. Khatoon and S. K. Dhawan, *J. Mater. Sci.*, 47 (2012) 2461
22. S. G. Pawar, S. L. Patil, M. A. Chougule, A. T. Mane, D. M. Jundale and V. B. Patil, *Int. J. Polym. Mater.*, 59 (2010) 777
23. A. Sakhri, F. X. Perrin, A. Benaboura, E. Aragon and S. Lamouri, *Prog. Org. Coat.*, 72 (2011) 473
24. U. M. Angst and B. Elsener, *Corros. Sci.*, 89 (2014) 307
25. Y. C. Chou, P. C. Lee, T. F. Hsu, W. Y. Huang, L. Z. Han, C. Y. Chuang, T. I. Yang and J.M. Yeh, *Polym. Compos.*, 35 (2014) 617
26. A. H. Navarchian, M. Joulazadeh and F. Karimi, *Prog. Org. Coat.*, 77 (2014) 347
27. D. M. Gurudatt and K. N. Mohana, *Ind. Eng. Chem. Res.*, 53 (2014) 2092
28. H. R. Zhang, J. X. Wang, X. X. Liu, Z. Wang and S. C. Wang, *Ind. Eng. Chem. Res.*, 52 (2013)

10172

29. S. P. Ali, C. Dehghanian and A. Kosari, *Corros. Sci.*, 85 (2014) 204
30. J. Y. Hu, D. Z. Zeng, Z. Zhang, T. H. Shi, G. L. Song and X. P. Guo, *Corros. Sci.*, 74 (2013) 35
31. J. A. Syed, S. C. Tang, H. B. Lu and X. K. Meng, *Ind. Eng. Chem. Res.*, 54 (2015) 2950
32. V. Karpakam, K. Kamaraj, S. Sathiyarayanan, G. Venkatachari and S. Ramu, *Electrochim. Acta*, 56 (2011) 2165

© 2015 The Authors. Published by ESG (www.electrochemsci.org). This article is an open access article distributed under the terms and conditions of the Creative Commons Attribution license (<http://creativecommons.org/licenses/by/4.0/>).